Complexity-Reduced Suboptimal Equalization with Monte Carlo Based MIMO Detectors

Guilherme C. G. Fernandes
Instituto Tecnológico de Aeronáutica
Embraer S.A.
São José dos Campos, SP, Brazil
gcosta@ita.br

Marcelo G. S. Bruno
Instituto Tecnológico de Aeronáutica
São José dos Campos, SP, Brazil
bruno@ita.br

***Abstract*—Optimal detection in multiple-input multiple-output (MIMO) frequency-selective systems is known to have exponential complexity in the number of transmitter antennas and channel length resulting from intersymbol interference. Several studies focus on suboptimal detectors, proposing trade-offs between computational complexity and bit error rate. In this paper, we model the detection problem using factor graphs and apply the sum-product algorithm to derive the optimal detector. Then we propose a novel suboptimal particle filter detector, based on sequential Monte Carlo, followed by a Markov chain Monte Carlo step to further enhance performance. The proposed algorithm exchanges the exponential complexity in channel length for a linear complexity in the number of particles and achieves better bit error rate than the linear minimum mean square error (LMMSE) detector.**

***Index Terms*—Equalization, MIMO detection, particle filter, Markov chain Monte Carlo, factor graphs**

I. Introduction

In multiple-input, multiple output (MIMO) communication systems, the transmitted symbols must be recovered from received signals that are corrupted by noise and intersymbol interference (ISI). The optimal solution for joint decoding of the transmitted symbols given the received signals recorded at all receiving antennas is the maximum *a posteriori* (MAP) detector which was proven, however, to have exponential complexity in the number of transmitter antennas and in the channel length resulting from ISI. That computational complexity motivates the development of suboptimal decoding approaches that make MIMO systems scalable [1].

The joint probability mass function (pmf), or density function (pdf), of the transmitted symbols can be represented by a factor graph (FG), as suggested in [2]- [4]. The sum-product algorithm (SPA), or *message-passing*, is the tool to obtain the marginal distributions required for decoding from a FG and results in the MAP detector if applied directly.

Suboptimal detectors can be derived using suitable approximations to the messages that flow through the FG in the SPA equations. In the linear minimum mean square error (LMMSE) approach [3], messages are approximated by multivariate Gaussian functions, whose mean vectors and covariance matrices are then propagated by the SPA. The Markov chain Monte Carlo (MCMC) detector [4] is based on the Gibbs sampler (GS), which uses conditional probability distributions to draw samples that converge to samples from the desired joint pmf and can be then averaged out.

In [5], we implemented the LMMSE and MCMC detectors in [4] and proposed a *hybrid MCMC/LMMSE detector* using the LMMSE solution to initialize the GS in the MCMC detector. The proposed hybrid algorithm achieved better bit error rate (BER) than the LMMSE and MCMC detectors individually. However, the Gaussian approximation fails to capture multiple peaks present in the joint pmf, whereas the GS presents the stall effect, i. e. the BER stops decreasing as the SNR increases. To overcome those limitations, motivated by [6] and [7], we propose a novel particle filter (PF) detector based on a sequential Monte Carlo (SMC) approximation of the functions in the SPA. The use of SMC approximations results in a significant reduction in the computational complexity of the SPA because the most costly operations in the algorithm have to be done only in a reduced set of transmitted symbols. Furthermore, we also propose a new *hybrid MCMC/PF detector*, where we perform the MCMC step initialized with the PF solution to further enhance performance.

The paper is divided in six sections. Sec. I is this Introduction. In Sec. II, we describe the signal model and its FG representation. In Sec. III, we present the exact equations for the MAP detector. In Sec. IV, we introduce the Monte Carlo based detectors. Simulations and detector comparison are shown in Sec. V and conclusions are presented in Sec. VI.

Notation: We denote scalars by a or A, vectors by $\mathbf{a}$ and matrices by $\mathbf{A}$. $(.)^T$ and $(.)^H$ denote matrix transpose and hermitian. $\mathbf{I}$ denotes the identity matrix. $[\mathbf{A}]_{i,j}$ is the element in the i-th row and j-th column of matrix $\mathbf{A}$. We denote random vectors by $\mathbf{A}$, which can be distinguished from deterministic matrices in context. We denote the probability of an event by $Pr(\mathbf{A})$. If $\mathbf{A}$ is discrete, we denote its pmf $Pr(\{\mathbf{A} = \mathbf{a}\})$ by $P(\mathbf{a})$. If $\mathbf{A}$ is continuous, we denote its pdf by $p(\mathbf{a})$. The expectation operator is denoted by $\mathbb{E}$.

II. Problem Statement

A. Signal Model of the Communication Problem

We assume a MIMO communication system with N_T transmitter and $N_R \geq N_T$ receiver antennas. The wireless chan-

The author's work was supported by CAPES and Fundação Casimiro Montenegro Filho.

978-9-0827-9703-9/19/$31.00 ©2019 IEEE

nel is linear, time-variant, frequency-selective with impulse response length L and presents Rayleigh fading. A stream of N_b uncoded bits is transmitted, each Q bits being mapped into $N_s = N_b/Q$ symbols according to some symbol alphabet $\mathcal{A}$ of size 2^Q. The symbols are transmitted over $N = N_s/N_T$ time instants, and received over $M = N + L - 1$ time instants due to ISI.

We assume the wireless channel has a coherence time of M, meaning that it will remain constant while the bit stream is being received. The channel is described by its taps $[\mathbf{H}_1 \cdots \mathbf{H}_L]$, where each $[\mathbf{H}_l]_{r,n} \in \mathbb{C}$ is the channel coefficient between the n-th transmitter and the r-th receiver antenna in the l-th reflection, drawn from a complex Gaussian distribution $\mathcal{CN}(0, 1)$. The channel estimation problem is not in the scope of this paper, thus all channel coefficients are considered *perfectly known* at the receiver.

Let s_i^n be the symbol at the n-th transmitter antenna at time instant i and $\mathbf{s}_i = [s_i^1 \cdots s_i^{N_T}]^T$ be the vector of all transmitted symbols at instant i. The received signal is then modeled by

$$\mathbf{y}_i = \sum_{l=1}^{L} \mathbf{H}_l \mathbf{s}_{i-l+1} + \mathbf{z}_i \tag{1}$$

where $\mathbf{y}_i = [y_i^1 \cdots y_i^{N_R}]^T$, y_i^r denotes the signal received by the r-th receiver antenna at instant i, and $\mathbf{z}_i$ is random white complex Gaussian noise, with $\mathbb{E}[\mathbf{Z}_i] = \mathbf{0}$ and $\mathbb{E}[\mathbf{Z}_i \mathbf{Z}_i^H] = \sigma_z^2 \mathbf{I}$.

The problem of interest is to obtain an estimate $\hat{\mathbf{b}}$ of all transmitted bits $\mathbf{b}$ given the collection $\mathbf{y} = \mathbf{y}_{1:M} = [\mathbf{y}_1^T \cdots \mathbf{y}_M^T]^T$ of all observations $\mathbf{y}_i$ using $P(\mathbf{b}|\mathbf{y})$. The MAP detector expression for each bit is given by

$$\hat{b}_{k,\text{MAP}} = \underset{b_k \in \{0,1\}}{\text{argmax}} \sum_{\mathbf{b}/\{b_k\}} P(\mathbf{b}|\mathbf{y}) = \underset{b_k \in \{0,1\}}{\text{argmax}} P(b_k|\mathbf{y}). \tag{2}$$

where $\sum_{\mathbf{b}/\{b_k\}}$ denotes summation over all variables in $\mathbf{b}$, except b_k. Since bits and symbols relate to each other deterministically, the bitwise detector in (2) can be expressed as an equivalent symbolwise detector based on $P(\mathbf{s}|\mathbf{y})$

$$\hat{s}_{i,\text{MAP}}^n = \underset{s_i^n \in \mathcal{A}}{\text{argmax}} \sum_{\mathbf{s}/\{s_i^n\}} P(\mathbf{s}|\mathbf{y}) = \underset{s_i^n \in \mathcal{A}}{\text{argmax}} P(s_i^n|\mathbf{y}), \tag{3}$$

where $\mathbf{s}$ represents the collection of all transmitted symbols.

B. Representation with Factor Graph

The joint probability functions $P(\mathbf{b}|\mathbf{y})$ or $P(\mathbf{s}|\mathbf{y})$ can be factorized and represented by a factor graph, so we can apply the SPA to calculate the marginals needed for detection in (2) and (3). Without loss of generality, applying Bayes' Law to the probability function $P(\mathbf{s}|\mathbf{y})$, we obtain

$$P(\mathbf{s}|\mathbf{y}) \propto p(\mathbf{y}|\mathbf{s}) P(\mathbf{s}). \tag{4}$$

Applying the chain rule to the likelihood function on the right side of (4), expanding $\mathbf{y}$ and $\mathbf{s}$ as the collection of all received and transmitted signals, and observing conditional independence properties of the received signal $\mathbf{y}_i$, we rewrite the likelihood function on the right as

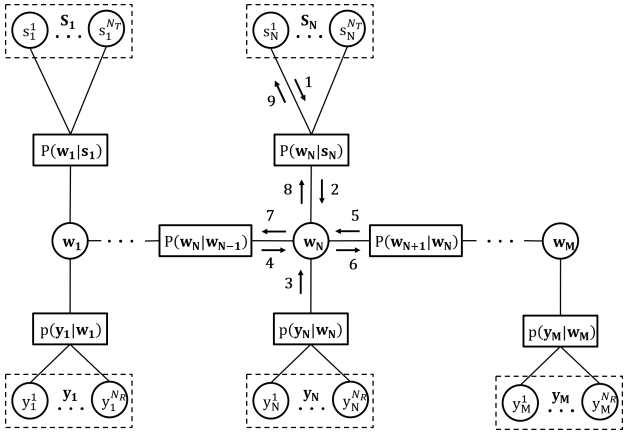

Fig. 1. Cycle-free FG resulting from factorization in (6).

$$p(\mathbf{y}|\mathbf{s}) = \prod_{i=1}^{M} p(\mathbf{y}_i|\mathbf{w}_i), \tag{5}$$

where $\mathbf{w}_i = [\mathbf{s}_{i-L+1}^T \cdots \mathbf{s}_i^T]^T$ is a state variable representing all transmitted symbols that influence the signal received at instant i. In order to obtain a cycle-free FG, we follow the lead in [3] and introduce indicator probability functions $P(\mathbf{w}_i|\mathbf{w}_{i-1})$ and $P(\mathbf{w}_i|\mathbf{s}_i)$, which evaluate to 1 when all the common symbols $\mathbf{s}_j$ between $\mathbf{w}_i$ and $\mathbf{w}_{i-1}$ or $\mathbf{s}_i$ match. Equation (5) is not modified if written as

$$\begin{aligned} p(\mathbf{y}|\mathbf{s}) = {} & p(\mathbf{y}_1|\mathbf{w}_1) P(\mathbf{w}_1|\mathbf{s}_1) \\ & \times \prod_{i=2}^{N} p(\mathbf{y}_i|\mathbf{w}_i) P(\mathbf{w}_i|\mathbf{w}_{i-1}) P(\mathbf{w}_i|\mathbf{s}_i) \\ & \times \prod_{i=N+1}^{M} p(\mathbf{y}_i|\mathbf{w}_i) P(\mathbf{w}_i|\mathbf{w}_{i-1}), \end{aligned} \tag{6}$$

which can be represented by the factor graph in Fig. 1, along with the messages of interest for each variable node and time instant i.

III. Optimal Detector

The sum-product algorithm (SPA), or message-passing, is described in [2]. Its output are the marginal probability functions for each variable node in the FG. If performed exactly, we obtain the exact *a posteriori* probability functions and can perform the MAP detection.

The exact application of the SPA consists of considering each message as a discrete pmf and evaluating it individually at each state. The resulting equations are given in [3]. All messages are normalized to a total probability of one in order to be valid pmf's.

The *a priori* knowledge of the symbol distribution is represented by message 1, or m_1, defined in Fig. 1, which is usually

considered uniform. Using the SPA expressions, message 2 defined in Fig. 1 is calculated as

$$m_2^{(i)}(\mathbf{w}_i) = \sum_{\mathbf{s}_i} P(\mathbf{w}_i|\mathbf{s}_i) \prod_{n=1}^{N_T} m_{1,n}^{(i)}(s_i^n). \tag{7}$$

Message 3 is calculated from the observation model as

$$m_3^{(i)}(\mathbf{w}_i) \propto \exp\left[-\left\|(\mathbf{y}_i - \bar{\mathbf{H}}_i \mathbf{w}_i)\right\|^2 / \sigma^2 \right] \tag{8}$$

where the matrix $\bar{\mathbf{H}}_i$, extended from (1), is given by

$$\bar{\mathbf{H}}_i = \begin{cases} [\mathbf{H}_i \cdots \mathbf{H}_1] & , i < L \\ [\mathbf{H}_L \cdots \mathbf{H}_1] & , L \leq i \leq N \\ [\mathbf{H}_L \cdots \mathbf{H}_{i-N+1}] & , i > N. \end{cases}$$

Messages 4 and 6 are calculated sequentially for $i = 1, \cdots, N$, forming the forward recursion

$$m_6^{(i)}(\mathbf{w}_i) = m_2^{(i)}(\mathbf{w}_i) m_3^{(i)}(\mathbf{w}_i) m_4^{(i)}(\mathbf{w}_i) \tag{9}$$

$$m_4^{(i)}(\mathbf{w}_i) = \sum_{\mathbf{w}_{i-1}} P(\mathbf{w}_i|\mathbf{w}_{i-1}) m_6^{(i-1)}(\mathbf{w}_{i-1}). \tag{10}$$

Messages 5 and 7 are also calculated sequentially for $i = M, \cdots, 1$, forming the backward recursion

$$m_7^{(i)}(\mathbf{w}_i) = m_2^{(i)}(\mathbf{w}_i) m_3^{(i)}(\mathbf{w}_i) m_5^{(i)}(\mathbf{w}_i) \tag{11}$$

$$m_5^{(i)}(\mathbf{w}_i) = \sum_{\mathbf{w}_{i+1}} P(\mathbf{w}_{i+1}|\mathbf{w}_i) m_7^{(i+1)}(\mathbf{w}_{i+1}). \tag{12}$$

Message 9 is calculated to finish the SPA. It has the following simplified expression [4]:

$$m_{9,n}^{(i)}(s_i^n) = \frac{1}{m_{1,n}^{(i)}(s_i^n)} \sum_{\mathbf{w}_i} P(\mathbf{w}_i|\mathbf{s}_i) m_5^{(i)}(\mathbf{w}_i) m_6^{(i)}(\mathbf{w}_i). \tag{13}$$

Finally, detection is done by calculating the marginal distribution of each symbol, $P(s_i^n|\mathbf{y})$, as the product $m_{1,n}^{(i)} m_{9,n}^{(i)}$, and finding the maximum according to (3). In some cases, it is interesting to perform *turbo processing* feeding back $m_{9,n}^{(i)}$ in $m_{1,n}^{(i)}$, as an improved *a priori* knowledge [4].

At each instant i, the messages whose argument is $\mathbf{w}_i$ require performing calculations for each of the $\mathcal{O}(2^{QLN_T})$ possible values assumed by $\mathbf{w}_i$, a set we denote as $\mathcal{W}_i$.

IV. Particle Detectors

In this work, the approach to obtain suboptimal detectors is to approximate the messages using particle methods. We propose a particle filter (PF) detector based on a sequential Monte Carlo approximation, followed by a MCMC detector initialized with the previously obtained solution.

A. Particle Filter Detector

A particle representation of a function $f(x)$ is a list of weighted particles $\mathcal{L} \triangleq \{(x^{(p)}, w^{(p)})\}$, for $p = 1$ to N_p, such as that $w^{(p)} \geq 0$ and $\sum_{p=1}^{N_p} w^{(p)} = 1$.

The particle filter (PF) detector is derived approximating the messages in the MAP equations (7) to (13). In the forward recursion, assuming $m_6^{(i-1)}$ is given, we represent it with N_p particles drawing samples $\mathbf{w}_{i-1}^{(p)}$ from it, with uniform weights. Message 4 is then calculated as

$$m_4^{(i)}(\mathbf{w}_i) \approx \sum_{p=1}^{N_p} P(\mathbf{w}_i|\mathbf{w}_{i-1}^{(p)}) w^{(p)} \propto \frac{1}{N_p} \sum_{p=1}^{N_p} \hat{m}_4^{(i)(p)}(\mathbf{w}_i). \tag{14}$$

We define $\hat{m}_4^{(i)(p)}$ as a *particle message* associated with $m_4^{(i)}$. It must be normalized to be a valid pmf. For each p, when calculating $\hat{m}_4^{(i)(p)}$, only the 2^{QN_T} states $\mathbf{w}_i = [\mathbf{s}_{i-L+1}^{T(p)}, \cdots, \mathbf{s}_{i-1}^{T(p)}, \mathbf{s}_i^T]^T$ will not be zero. We denote the set containing those states $\mathbf{w}_i$ as $\mathcal{W}_{i,F}^{(p)}$.

The second step of the forward recursion is the calculation of $m_6^{(i)}$. Using (9) and (14),

$$\begin{aligned} m_6^{(i)}(\mathbf{w}_i) &\approx m_2^{(i)}(\mathbf{w}_i) m_3^{(i)}(\mathbf{w}_i) \frac{1}{N_p} \sum_{p=1}^{N_p} \hat{m}_4^{(i)(p)}(\mathbf{w}_i) \\ &= \frac{1}{N_p} \sum_{p=1}^{N_p} m_2^{(i)}(\mathbf{w}_i) m_3^{(i)}(\mathbf{w}_i) \hat{m}_4^{(i)(p)}(\mathbf{w}_i) \\ &= \frac{1}{N_p} \sum_{p=1}^{N_p} \hat{m}_2^{(i)(p)}(\mathbf{w}_i) \hat{m}_3^{(i)(p)}(\mathbf{w}_i) \hat{m}_4^{(i)(p)}(\mathbf{w}_i) \\ &\propto \frac{1}{N_p} \sum_{p=1}^{N_p} \hat{m}_6^{(i)(p)}(\mathbf{w}_i), \end{aligned} \tag{15}$$

where $\hat{m}_6^{(i)(p)}$ must be normalized to a valid pmf. Particle messages $\hat{m}_2^{(i)(p)}$ and $\hat{m}_3^{(i)(p)}$ are defined as assuming the same values of (7) and (8), respectively, if $\mathbf{w}_i \in \mathcal{W}_{i,F}^{(p)}$, and zero otherwise, since $\hat{m}_4^{(i)(p)}$ is zero for those states.

All $\hat{m}_6^{(i)(p)}$ must be averaged elementwise in order to obtain $m_6^{(i)}$ and proceed with the forward recursion. The initial message $m_6^{(1)}$ is calculated using the MAP equations.

The backward recursion requires sampling from $m_7^{(i+1)}$ in order to obtain particles $\mathbf{w}_{i+1}^{(p)}$. Following (14) and (15), we define particle messages $\hat{m}_5^{(i)(p)}$ and $\hat{m}_7^{(i)(p)}$ as

$$\hat{m}_5^{(i)(p)}(\mathbf{w}_i) \propto P(\mathbf{w}_{i+1}^{(p)}|\mathbf{w}_i) \tag{16}$$

$$\hat{m}_7^{(i)(p)}(\mathbf{w}_i) \propto \hat{m}_2^{(i)(p)}(\mathbf{w}_i) \hat{m}_3^{(i)(p)}(\mathbf{w}_i) \hat{m}_5^{(i)(p)}(\mathbf{w}_i), \tag{17}$$

which evaluate to zero unless $\mathbf{w}_i = [\mathbf{s}_{i-L+1}^T, \mathbf{s}_{i-L+2}^{T(p)}, \cdots, \mathbf{s}_i^{T(p)}]^T$, which we define as $\mathbf{w}_i \in \mathcal{W}_{i,B}^{(p)}$. In order to proceed with the backward

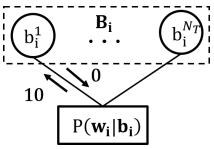

Fig. 2. Factor graph node modification for bitwise detection in MCMC.

recursion, all $\hat{m}_7^{(i)(p)}$ and $\hat{m}_5^{(i)(p)}$ are averaged elementwise. The initial message $m_7^{(M)}$ is calculated using the MAP equations. Similarly to the forward recursion, the backward recursion has computational complexity $\mathcal{O}(N_p 2^{QN_T})$.

The last approximation is done for $m_{9,n}^{(i)}$ (13). We avoid the summation over $\mathcal{W}_i$ using a particle representation either for $m_5^{(i)}$ or $m_6^{(i)}$. Drawing N_p particles from $m_6^{(i)}$, we define

$$\hat{m}_{9,n}^{(i)(p)}(s_i^n) \propto \frac{1}{m_{1,n}^{(i)}(s_i^n)} P(\mathbf{w}_i^{(p)}|\mathbf{s}_i) m_5^{(i)}(\mathbf{w}_i^{(p)}), \tag{18}$$

where $P(\mathbf{w}_i^{(p)}|\mathbf{s}_i)$ evaluates to one only for $s_i^n = s_i^{n,(p)}$. All $\hat{m}_{9,n}^{(i)(p)}$ are averaged to obtain $m_{9,n}^{(i)(p)}$.

The advantage of this method is that all particle messages whose argument is $\mathbf{w}_i$, for $p = 1$ to N_p, are evaluated with complexity $\mathcal{O}(N_p 2^{QN_T})$, eliminating the exponential complexity in L present in the optimal detector. The averaging of particle messages $\hat{m}_6^{(i)(p)}$ and $\hat{m}_7^{(i)(p)}$ still has to be done with complexity $\mathcal{O}(2^{QLN_T})$, but this is a much simpler operation than those in (7) and (8), thus having a smaller computational time. The initialization steps in both recursions do not compromise the complexity, since $\mathbf{w}_1 = \mathbf{s}_1$ and $\mathbf{w}_M = \mathbf{s}_N$. The number of particles N_p can be viewed as a parameter that can adjust the trade-off between BER performance and computational complexity.

B. MCMC-based Hybrid Detector

The MCMC detector is based on the Gibbs sampler [8], [9]. Following the approach in [4], decoding is done using the bitwise detector in (2), whose FG requires changing the symbol nodes in Fig. 1 for bit nodes as in Fig. 2. The GS approximates the desired pmf iteratively generating R samples from $P(\mathbf{b}|\mathbf{y})$ by drawing samples from all conditional probabilities $P(b_k|\mathbf{b}/\{b_k\}, \mathbf{y})$. Given the *a priori* distribution of bits $\hat{m}_{0,k}^{(i)(r)}(b_k)$, the equations needed to draw a sample b_k are given by [4]

$$\hat{m}_3^{(i)(r)}(b_k) \propto \exp\left[-\left\|(\mathbf{y}_i - \bar{\mathbf{H}}_i \mathbf{w}_i^{(r)}(b_k))\right\|^2 / \sigma^2\right] \tag{19}$$

$$\hat{m}_7^{(i)(r)}(b_k) \propto \hat{m}_3^{(i)(r)}(b_k) \hat{m}_5^{(i)(r)}(b_k) \tag{20}$$

$$\hat{m}_5^{(i)(r)}(b_k) \propto \hat{m}_7^{(i+1)(r)}(b_k) \tag{21}$$

$$\hat{m}_{10,k}^{(i)(r)}(b_k) \propto \hat{m}_3^{(i)(r)}(b_k) \hat{m}_5^{(i)(r)}(b_k) \tag{22}$$

$$b_k^{(r)} \sim m_{0,k}^{(i)}(b_k) \hat{m}_{10,k}^{(i)(r)}(b_k). \tag{23}$$

In (19) to (23), the index k corresponds to the k-th transmitted bit, whereas i is the time instant when this bit was transmitted and r is the index of the r-th iteration of the GS.

The samples are drawn from $k = 1$ to N_b and then from $r = 1$ to R. After all samples are drawn, we decode the correct bits "burning" the first b particle messages $\hat{m}_{10,k}^{(i)(r)}$ and averaging the remaining, for $r = b + 1$ to R. $\mathbf{w}_i^{(r)}(b_k)$ is the state of symbols modulated from a subsequence of the sequence of bits $[b_0^{(r)}, \cdots, b_{k-1}^{(r)}, b_k, b_{k+1}^{(r-1)}, \cdots, b_{N_b}^{(r-1)}]$. For each bit and GS iteration r, (19) to (22) are performed L times [4], which gives a total complexity for decoding each symbol of $\mathcal{O}(QLR)$.

The GS requires an initial state for the bits, which is usually chosen at random. However, encouraged by [10], we apply to our equalization problem an initialization coming from other suboptimal detector, resulting in the hybrid detector.

V. Results and Discussion

We compared the BER performances of the suboptimal and the MAP detectors via Monte Carlo simulations. The basic simulation setup is the following: $N_R = 2, N_T = 2$ and $L = 2$, with BPSK modulated symbols. The bits are transmitted in batches of coherence time 16, meaning that the channel coefficients drawn independently from a $\mathcal{CN}(0, 1)$ distribution remain constant only during the transmission of $16QN_T$ bits. The PF detector is set initially with $N_p = 40$, and the Gibbs sampler with $R = 15$ and $b = 5$.

Figure 3 presents the comparison between the following detectors: MAP, PF, hybrid MCMC/PF, LMMSE, hybrid MCMC/LMMSE and pure MCMC. At low signal-to-noise ratio (SNR) regimes, all detectors present similar performance. As the SNR increases, the BER of both the PF and LMMSE detectors decreases, with the PF detector curve occupying the region between the LMMSE and MAP curves. The MCMC detector, however, reaches a BER floor due to the Gibbs sampler stall effect [11].

The fact that the PF detector has complexity $\mathcal{O}(N_p 2^{QN_T})$ compared to $\mathcal{O}(L^3 N_T^3)$ and $\mathcal{O}(2^{QLN_T})$ for the LMMSE and the MAP detectors, respectively, makes it an attractive algorithm based on a trade-off between performance and computational cost. The performance gains achieved by the PF detector compared to the LMMSE detector are explained by the ability of the SMC approach to better approximate any probability distribution, as opposed to the Gaussian approach, which fails to capture the multimodality of the joint probability distribution of the symbols in the constellation.

On the other hand, compared to the pure MCMC detector, the PF detector presents much better BER and, more importantly, did not exhibit the stalling effect in the simulated SNR range. Conversely, the hybrid MCMC/PF and MCMC/LMMSE detectors perform very similarly and better than any of the three suboptimal detectors independently, but just slightly better than the PF detector. Given that the MCMC

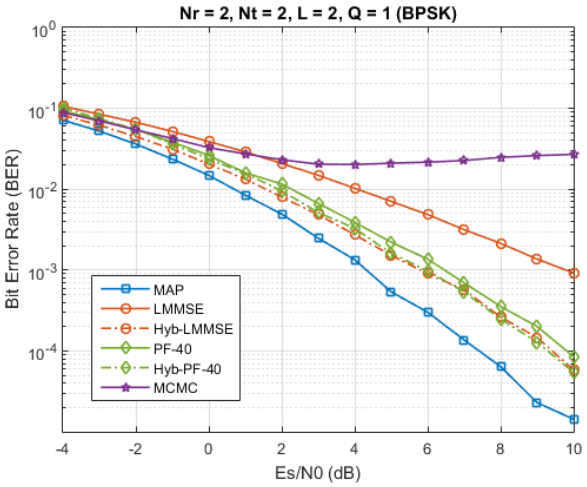

Fig. 3. BER performance of different suboptimal detectors, BPSK

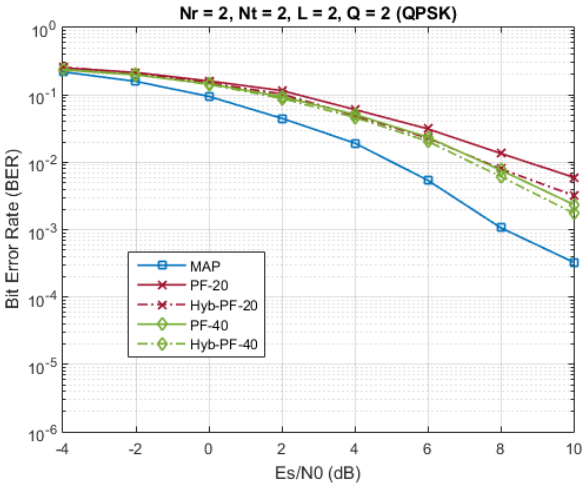

Fig. 5. Particle filter detectors with different N_p, QPSK

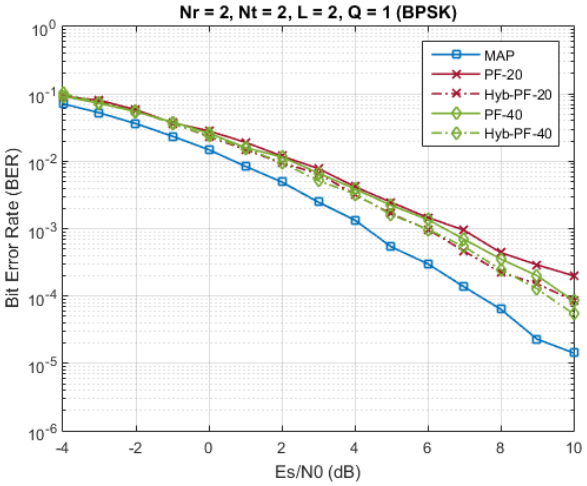

Fig. 4. Particle filter detectors with different N_p, BPSK

step increases the complexity with a $\mathcal{O}(QLR)$ factor and the gains are modest compared to the PF detector, the latter still continues to be an attractive option.

Finally, Fig. 4 and 5 depict the PF detector performance for BPSK and QPSK modulations, with $N_p = 20$ and 40. Increasing the number of particles improves the BER, as expected in a Monte Carlo method. The gain from increasing N_p is more significant in the QPSK scenario, since a modulation with more symbols presents more peaks and is better represented by Monte Carlo approximations with more particles.

VI. Conclusion

In this paper, we applied a factor graph formulation to solve the problem of equalization of a MIMO frequency-selective channel and derived a particle filter detector by proposing suitable Monte Carlo approximations to the SPA messages over the FG. Unlike the optimal MAP detector which has exponential complexity in the channel length, the proposed PF detector exhibits linear complexity in the number of particles, which can be tuned to achieve different levels of suboptimal BER. The BER performance of the proposed PF detector compares favorably to the LMMSE detector based on Gaussian approximations of the SPA messages. Further improvements in detection performance can be achieved by using an MCMC detector initialized with the output of either the PF or the LMMSE detectors. The hybrid detectors eliminate the stall effect seen in pure MCMC detectors at high SNR but, in our simulations, the hybrid MCMC/PF detector did not show any statistically significant difference in performance compared to the hybrid MCMC/LMMSE detector.

References

[1] S. Yang and L. Hanzo, "Fifty Years of MIMO Detection: The Road to Large-Scale MIMOs," *IEEE Comm. Surv. Tut.*, vol. 17, pp. 1941-1988, 2015.

[2] F. R. Kschischang, B. J. Frey and H. A. Loeliger, "Factor Graphs and the Sum-Product Algorithm," *IEEE Trans. Inform. Theory*, vol. 47, no. 2, pp. 498-519, Feb. 2001.

[3] B. Etzlinger, W. Haselmayr and A. Springer, "Equalization Algorithms for MIMO Communication Systems Based on Factor Graphs," *in Proc. IEEE Int. Conf. on Comm. (ICC 2011)*, June 2011.

[4] B. Etzlinger, W. Haselmayr and A. Springer, "Message Passing Methods for Factor Graph Based MIMO Detection," *Wireless Advanced*, pp. 132-137, June 2011

[5] G. C. G. Fernandes and M. G. S. Bruno, "Hybrid MCMC and LMMSE Detector for MIMO Frequency-Selective Channels," *in Anais do XXXVI Simpósio Brasileiro de Telecomunicações e Processamento de Sinais (SBrT 2018)*, pp. 176-180 Sep. 2018.

[6] J. Dauwels, S. Korl and H. A. Loeliger, "Particle Methods as Message Passing," *Proc. IEEE Int. Symp. on Inf. Theory*, July 2006.

[7] C. J. Bordin and M. G. S. Bruno, "Particle Filters for Joint Blind Equalization and Decoding in Frequency-Selective Channels," *in IEEE Trans. Signal Processing*, vol. 56, no. 6, pp. 2395-2405, June 2008.

[8] A. Doucet and X. Wang, "Monte Carlo Methods for Signal Processing," *IEEE Sig. Proc. Mag.*, vol. 22, pp. 152-170, Nov. 2005.

[9] D. Gamerman, *Markov Chain Monte Carlo: Stochastic Simulation for Bayesian Inference*. Chapman and Hall, 1997.

[10] X. Mao, P. Amini and B. Farhang-Boroujeny, "Markov Chain Monte Carlo MIMO Detection Methods for High Signal-to-Noise Ratio Regimes," *IEEE GLOBECOM*, pp. 3979-3983, Nov. 2007.

[11] S. Akoum, R. Peng, R. R. Chen and B. Farhang-Boroujeny, "Markov Chain Monte Carlo Detection Methods for High SNR Regimes," *Proc. IEEE Int. Conf. on Comm. (ICC 2009)*, June 2009.